Force Measurements on Single Molecular Contacts through Evanescent Wave Microscopy

Giovanni Zocchi
Department of Physics and Astronomy, University of California Los Angeles, Los Angeles, California 90095-1547 USA

ABSTRACT We introduce a new method to apply controlled forces on single molecules. The motion of a micron-sized bead attached to a solid surface through a single molecular contact is tracked by evanescent wave microscopy as a force is exerted through a flow. We report measurements of the streptavidin-biotin bond rupture force obtained with this technique. We also obtain detailed measurements of the balance of forces involved in detaching an adhering bead with a flow. A small lateral force translates into a much bigger normal force on the attachment point. This effect is relevant for the interpretation of common cell adhesion assays.

INTRODUCTION

Progress in detecting and manipulating single molecules (in particular biological macromolecules) is permitting to exert controlled forces on these systems and study their dynamics (see the issue of *Science*, March 12, 1999). The groundbreaking work on motor proteins, via optical trapping (Howard et al., 1989; Block et al., 1990; Svoboda et al., 1993), demonstrated the feasibility of extracting dynamical information from single-molecule experiments, and was followed by a series of studies on the mechanical and dynamical properties of processive enzymes, long DNA strands, and ligand-receptor binding. Thus, the motion of kinesin along the microtubule was visualized directly by fluorescence (Vale et al., 1996), load-velocity curves were obtained for RNA polymerase (Yin et al., 1995; Wang et al., 1998) and kinesin by optical trapping (Svoboda and Block, 1994; Meyhofer and Howard, 1995; Coppin et al., 1997; Kojima et al., 1997). More recently, the rotation of F1 ATPase was visualized by fluorescence (Noji et al., 1997; Yasuda et al., 1998). Force-extension curves were obtained for long ($\sim$10 μm) DNA strands using micromechanical techniques (Smith et al., 1992, 1996; Cluzel et al., 1996), and the force necessary to separate single molecular contacts was measured for several systems, including biotin-avidin (Florin et al., 1994; Merkel et al., 1999), complementary nucleotides (Boland and Ratner, 1995; Essevaz-Roulet et al., 1997), and antibody-antigen (Hinterdorfer et al., 1996; Allen et al., 1999). Also recently, the giant protein titin was reversibly unfolded by mechanically pulling on it (Kellermayer et al., 1997; Tskhovrebova et al., 1997; Rief, 1997; Viani et al., 1999).

A parallel development concerned atomic force microscopy (AFM) imaging of molecular processes (Drake et al., 1989). In particular, the introduction of the tapping mode (Hansma et al., 1994) allowed the detection of nanometer scale conformational motion (Radmacher et al., 1994); here, one tries to minimize the force applied to the molecule.

Most mechanical studies in which the displacement was measured, as well as the force, have so far been performed on systems such that the overall displacement was of the order of microns: λ-DNA, processive enzymes, and titin. Similar experiments on the 1-nm scale conformational motion of nonprocessive enzymes are challenging. One difficulty is exemplified by the two most successful methods to measure single molecules rupture forces: the micropipette-supported biomembrane probe developed by Evans and collaborators (Merkel et al., 1999) and the AFM. The former is very compliant and therefore ideally suited to work with single molecular attachments; narrow distributions of rupture forces which reflect only single-bond events have been obtained. But for the same reason, the method is not suited to investigate nanometer scale motion of the molecular attachment. In contrast, the less compliant AFM is in principle more suited to extract spatial information, but it is more difficult to maintain a single molecular attachment for an extended time; consequently, most studies have so far relied on multiple attachment points, and obtained broad rupture force distributions, including multiple-bonds events.

In view of the above, it seems useful to also explore alternative techniques. We have been developing one such alternative, based on evanescent wave microscopy. We have demonstrated that the method is capable of detecting nanometer scale motion related to conformational changes of globular proteins fixed to a surface (Zocchi, 1997). Here, we show that the same technique can be used for quantitative force measurements at the single molecular contact level.

This paper contains two main points: we demonstrate quantitative force measurements with this method, and we obtain a direct measurement of why, in the geometry of a bead attached to a surface through few molecular contacts (which is the same geometry as an adhering cell), a com-

Received for publication 16 October 2000 and in final form 22 August 2001.

Address reprint requests to Dr. Giovanni Zocchi, University of California-Los Angeles, Department of Physics and Astronomy, 405 Hilgard Avenue, Box 951547, Los Angeles, CA 90095-1547. Tel.: 310-825-4018; Fax: 310-206-5668; E-mail: zocchi@physics.ucla.edu.

0006-3495/01/11/2946/08 $2.00

paratively small lateral force is sufficient to break the bonds. The latter point is relevant to the interpretation of cell adhesion assays and has previously been investigated theoretically by Chang and Hammer (1996); our measurements corroborate the results from their model, and further address the question of what is really the quantity (or quantities) measured in the common adhesion assays.

Experimental system

Our experimental system consists ideally of a micron-sized bead attached to a glass surface through a single molecular contact. This introduces a constraint in the Brownian motion of the bead, which can only "rock" around this pivotal point. We measure the vertical (i.e., perpendicular to the glass surface) fluctuations of the center of mass (CM) of the bead (which correspond to this rocking motion) through an evanescent wave-scattering technique which provides nanometer scale resolution (Prieve and Frey, 1990; Prieve and Walz, 1993; Zocchi, 1996). Apart from the constraint of the attachment point, the bead is in a field of force because of its interaction with the solid surface. At distances beyond a Debye screening length (1 to 2 nm in our system, depending on conditions) this interaction is well described by a Derjaguin–Landen–Verwey–Overbeek (DLVO) potential (Israelachvili, 1991), the sum of a repulsive electrostatic interaction (the bead and glass surfaces are negatively charged) and an attractive Van der Waals force. The DLVO potential has a secondary minimum typically at separations of a few nanometers (the primary minimum being at contact, i.e., sticking), and we have previously shown (Singh-Zocchi et al., 1999) that we can prepare the system so that the bead, attached at one point, still performs a constrained Brownian motion in this secondary minimum. This is because the surfaces are rough at the nanometer scale, so that the bead can be attached at one point while the "effective distance" of the surfaces h (i.e., the position of the bead's CM above the flat surface minus the average radius of the bead) is still many nanometers (Fig. 1 *a*). This setup can be used to exert a controlled force on the attachment point. First, the interaction potential is deduced from a recording of the vertical Brownian motion of the bead. Then a flow is applied parallel to the glass plate; the horizontal drag force F_h on the bead produces a torque around the attachment point, which pushes the bead against the plate, i.e., against the repulsive barrier of the DLVO potential (Fig. 1 *b*). Noting the new equilibrium height of the bead, we obtain (from the slope of the potential at that height) the vertical force F_v on the attachment point, which corresponds to the applied flow. Because of the geometry, there is a lever arm effect: the horizontal drag force F_h acts with a lever arm, with respect to the attachment point, of order R (the radius of the bead), whereas the vertical force F_v, because of the repulsive potential barrier, acts with a lever arm (x), which is only the horizontal displacement of the bead's CM with respect to the attachment point. Thus, at equilibrium $F_v = R/x\ F_h \gg F_h$ so the force on the attachment point is essentially F_v, which is the measured quantity. In our setup F_v/F_h is typically >10.

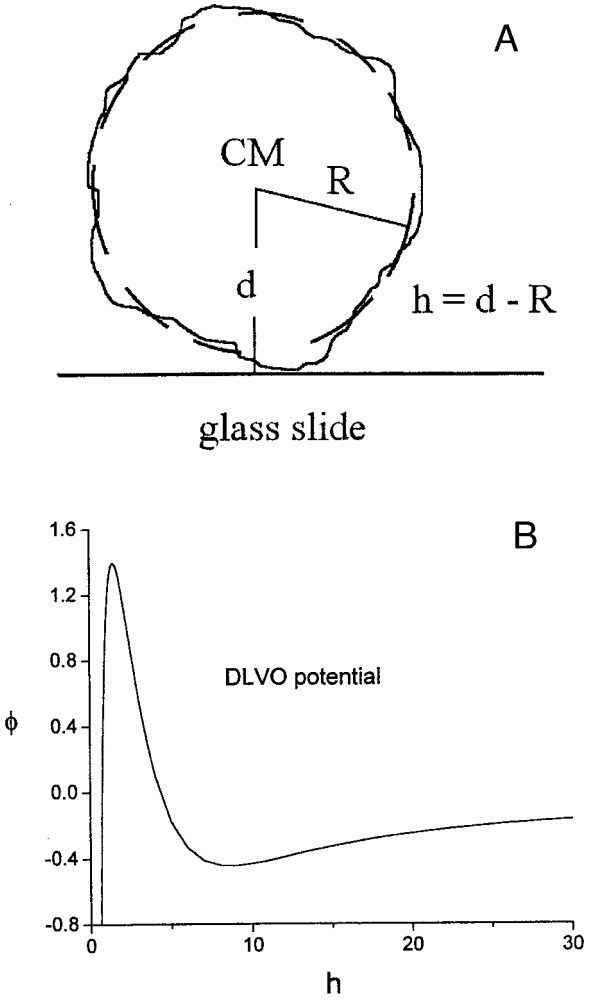

FIGURE 1 (*a*) Sketch of a bead attached to the slide at one point. The surface roughness is greatly exaggerated. (*b*) Sketch of the interaction potential (DLVO potential) between bead and slide (arbitrary units). The primary minimum is at contact ($h = 0$), but the system can be prepared with the bead, attached at one point, sitting in the secondary minimum. This is the part of the potential mapped in the measurements of Fig. 2.

This is one of the main points of this paper: we present detailed measurements of this effect, which explains why it is possible to detach a bead (or an adhering cell) with a comparatively small force. As pointed out by Chang and Hammer (1996), this effect must be considered when interpreting the outcome of cell adhesion assays. Quantifying cell adhesion is of considerable importance in cell biology and medicine, because adhesion plays a central role in regulating cell growth and function. The two most common assays are based on washing off adhering cells with a (lateral) flow, or removing them with a normal (body) force (by centrifugation) (Loster and Horstkorte, 2000). As noted

in Chang and Hammer (1996), the two methods lead to very different detachment forces, because of the aforementioned effect. Here we also show that even with uniform beads (exhibiting less variability in size and shape than a sample of cells), the ratio F_v/F_h can vary by more than one order of magnitude from bead to bead; correspondingly, for any individual bead the flow needed to detach it is not a good measure of the strength of the bond, being instead critically dependent on the local geometry of the attachment points. In the case of adhesion assays, even for a measurement averaged over an ensemble of cells, it is questionable whether the flow at detachment (or the fraction of cells surviving a certain flow, or similar measures) always bears a relation to the strength of the bonds, or the number of bonds, or the surface of contact. Some very different property of the cell, e.g., the local rigidity around the attachment point, may have a bigger effect on the measurement. Even assays which use a normal force may not be immune to this problem because the rigidity of the cell membrane may introduce a similar (albeit numerically smaller) lever arm effect (R. Bruinsma, private communication).

We now give more details about the experimental setup. The flow chamber is built with a microscope slide and cover glass (Fisher Scientific, Pittsburgh, PA) separated by 125-μm thick spacers and glued with wax. The glass was previously cleaned with soap in an ultrasound bath, left for 20 min in a 1:1:5 solution of H_2SO_4, H_2O_2, and H_2O at 60°C, rinsed with deionized water and blow-dried with nitrogen. At one end of the flow chamber, we glue a disposable pipette tip connected to a syringe (Hamilton Co., Reno, NV) which creates the flow by suction. The piston of the syringe is controlled by a stepping motor. At the other end of the chamber, we glue a well formed by an O-ring, which serves as the reservoir of solution. The flow chamber's dimensions are: width $\approx$ 11 mm, thickness $\approx$ 125 μm, volume $\approx$ 30 μl. This chamber is coupled with immersion oil to the hypotenuse of a Dove prism; the prism serves the purpose of bringing a laser beam (20 mW He-Ne laser) to be reflected at the bottom of the chamber (at the glass-solution interface) at an incidence angle beyond the critical angle for total internal reflection. This creates an evanescent wave in the halfspace above the glass-solution interface, characterized by a penetration depth $\Delta \approx 86$ nm for the measurements reported here. If a bead is present close to the glass surface, it scatters some of this light, and the scattered intensity $I_{sc} = I_c\exp(-h/\Delta)$ is a measure of the height h of the bead above the surface; I_c is the scattered intensity at contact. The scattered light is collected through a microscope objective (53×, NA 0.90) and focused onto a photodiode; the signal is recovered through a lock-in detection scheme. A computer controls the data acquisition and the flow pump. Samples are prepared as follows. First, a mixture of biotinilated bovine serum albumin (B-BSA) and unmodified BSA (both from Sigma, St. Louis, MO) in the ratio $1{:}2 \times 10^4$ is introduced in the flow chamber and left for ~15 min; the mix is in phosphate-buffered saline (PBS) at pH 6, at a BSA concentration of 1 mg/ml. A suspension of beads (4.5-μm diameter polystyrene spheres from Polysciences, Inc., Warrington, PA) with total surface area similar to the chamber's (~4 cm^2) is prepared in a similar mixture, only the B-BSA to BSA ratio is $1{:}\ 5\times10^4$. This step prepares BSA-covered surfaces with a low density (estimated at 1 molecule per μm^2) of B-BSA. After washing, the beads are stored in PBS pH 7.4 (plus BSA 0.1 mg/ml), whereas the chamber is filled with a solution of streptavidin (Sigma) 1 pmol/μl in PBS at pH 7.4 (and BSA 0.1 mg/ml). For most experiments, the streptavidin was partially blocked with biotin (by mixing them in the molar ratio 1: 1) before use. After 10 min, the chamber is washed several times and is ready for use. A dilute suspension of the beads is introduced, in PBS/6 (PBS diluted by 6) at pH 7.4 containing 20 μM Tween; then we start looking for beads showing promise of being anchored to the slide by a single streptavidin-biotin bond.

With this preparation, most beads in the chamber (>90%) are not bound at any given time; increasing the product of the concentrations of B-BSA on the two surfaces (beads and chamber) by a factor of 10 results in most beads getting anchored through multiple attachment points (as judged by the vertical fluctuations of the beads); decreasing this product by a factor of 10 results in bead attachment being so rare as to make the experiments impractical. In control experiments where either the streptavidin or the B-BSA step on one surface was omitted, beads were found to be always free, except occasionally a bead would be completely stuck (no measurable fluctuations), presumably on a damaged part of the surface. However, similar experiments with glass beads revealed a significant amount of nonspecific sticking; therefore we finally performed the experiments with polystyrene beads.

Measurements

To demonstrate the method, we now present measurements of the force required to detach single biotin-streptavidin contacts. The procedure is as follows. First we select a candidate bead according to the following criteria: (1) the bead is attached (not swept off by a (slow) flow); (2) the bead shows vertical fluctuations of at least 3–4 nm: this eliminates beads with several (specific or nonspecific) attachment points; also, we need fluctuations of at least a few nanometers to be able to determine the interaction potential reliably; and (3) the bead reacts to a (slow) flow in the expected way, i.e., it moves closer to the plate when the flow is switched on and recovers its original state (average height, root-mean-square fluctuations) when the flow is turned off. Sometimes beads find an additional attachment point when they are forced down toward the plate. These beads do not come back to their original state in the absence of flow and are discarded.

Note that these measured vertical fluctuations correspond to a rocking motion of the bead around the attachment point (i.e., the center of the bead moves along an arc of a circle); these are not vertical elastic deformations of the attachment point. A bead attached by one point can pivot in any direction (two degrees of freedom), and exhibits the largest fluctuations; a bead attached by two points can pivot only around a line joining the points

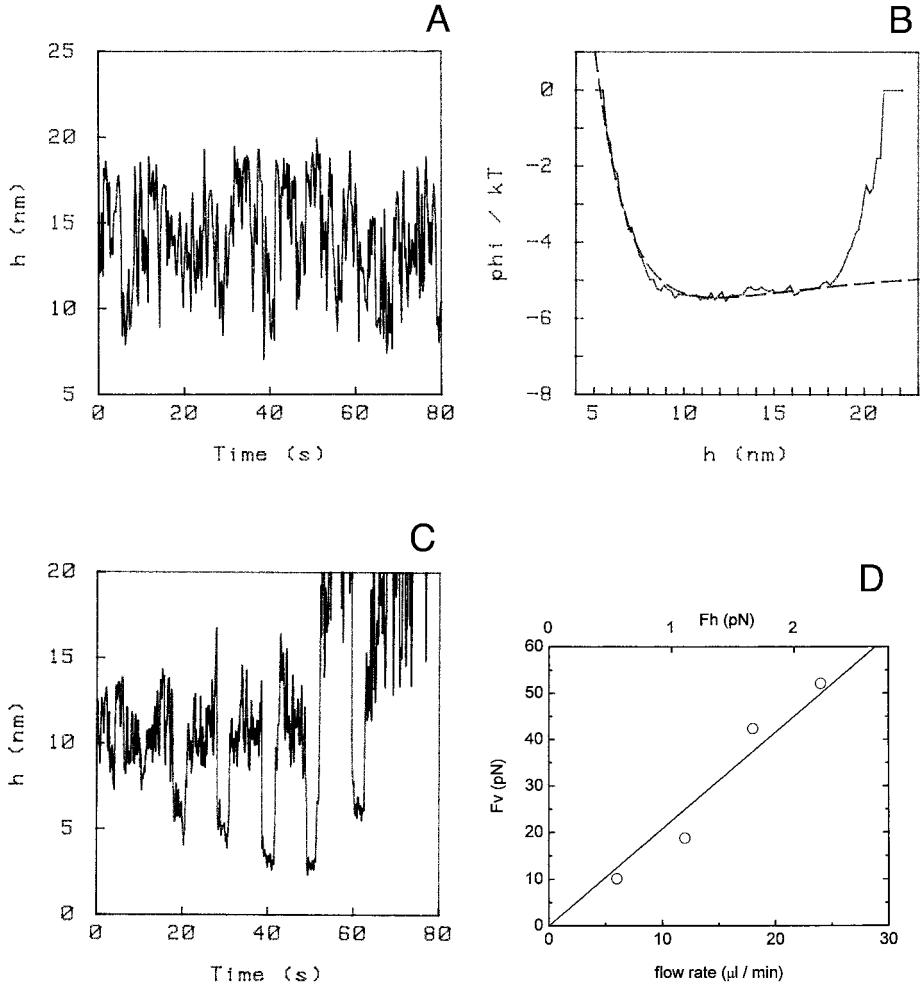

FIGURE 2 (*a*) Time course of the vertical fluctuations of a bead tethered by a single molecular attachment. The vertical motion is cutoff at $h \approx 20$ nm, reflecting the constraint imposed by the bond. (*b*) The interaction potential $\phi(h)$ between bead and slide derived from the measurement in *a*. When compared with a DLVO fit (*dashed line*), the constraint imposed by the attachment point is evident. (*c*) Time series showing the effect on the bead's vertical position of a series of flows with increasing velocity (6, 12, 18, 24, and 30 μl/min) used to calibrate the corresponding force imposed on the attachment point. The flows have a duration of 3 s and are 10 s apart. The first flow starts at $t \approx 17$ s. In a flow, the bead is pushed toward the slide, against the repulsive barrier of the DLVO potential (*b*); accordingly, the fluctuations are reduced. The new equilibrium position of the bead in the flow is determined from this recording and used to calculate the corresponding vertical force according to the potential in *b*. The attachment point of this particular bead broke during the fourth flow (corresponding, in this case, to a force of 51 pN), as seen by the much bigger vertical fluctuations (reaching up to ~50 nm, although not shown in the figure). Even after breaking the most constraining bond, this bead remained loosely connected (through a much longer tether) to the slide, as seen by the effect of the fifth flow. (*d*) The calibration obtained from *c*. The vertical force F_v (in pN) and the flow rate (in μl/min) are measured. The horizontal force F_h is calculated. For this bead, $F_v/F_h \approx 23$.

(one degree of freedom), and a bead attached by three or more points cannot pivot at all (unless all points are essentially aligned). We find experimentally that beads exhibiting 3–4 nm vertical fluctuations are most probably attached by a single point.

With our preparation method, only ~1 in 10 beads pass these selection criteria. Once a bead is selected, we take a 3-min time series (acquisition rate 64 Hz) of the vertical fluctuations (Fig. 2 *a*), build the corresponding histogram of the vertical position h and calculate the potential $\phi(h)$ according to $P(h) \alpha \exp(-\phi(h)/kT$ where $P(h)$ is the probability of finding the bead at height h (Fig. 2 *b*). To obtain a reference height we need to introduce a reference intensity of the scattered light, such as I_c, the intensity "at contact," i.e., with the bead collapsed on the plate. If we did not rip off the bead in the course of the measurement (to measure the detachment force), we could measure I_c for any individual bead by collapsing the bead on the plate in a high ionic strength solution at the end of the measurement (Singh-Zocchi et al., 1999).

Instead, we measured the range and average value of I_c on a test sample where the beads were collapsed on the slide in high ionic strength solution. We found that the range of I_c is narrow enough (corresponding to uniformly sized beads) that picking any value within this range does not affect the force calibration significantly, i.e., we checked numerically that the force calibration, described below, is not sensitive to the precise value of I_c within this range. In the end, for each bead in the present measurements we assigned a value of I_c, within the range determined from the test sample, such that the repulsive barrier of the corresponding measured interaction potential falls at $h \simeq 5 \div 6$ nm, consistent with the position of the barrier (approximately the distance of closest approach of the beads to the plate) which we obtain from the test sample (before collapsing the beads on the slide).

Next, we take a second time series (typically 90 s at 16 Hz) during which progressively faster flows are switched on and off for the purpose of calibrating the corresponding applied force (Fig. 2 *c*). For most of the measurements presented here, we used a sequence of 5 flow rates (6, 12, 18, 24, 30 μl/min) of the duration of 3 s with 7-s intermissions. The equilibrium position of the bead in each flow is determined "by hand" on the computer screen, and the corresponding vertical forces F_v are calculated from a fit to the measured potential. The fit for the potential is a DLVO form

$$\phi(h) = A_1 e^{-h/\delta} - \frac{A_2}{h} + A_3 \qquad (1)$$

(*dotted line* in Fig. 2 b) (Israelachvili, 1991); the first term describes the electrostatic repulsion, which decays exponentially because of the screening effect of ions in solution (δ is the Debye length; for the conditions of these measurements $\delta \approx 1.87$ nm); the second term describes the Van der Waals attraction, the exponent of the power law resulting from the geometry (sphere against a plane). The constants A_1 and A_2, both proportional to the radius of the sphere, contain the surface charge and Hamaker constant, respectively; A_3 is the arbitrary additive constant to the energy. Once A_1 and A_2 are determined by the fit, the vertical force F_v corresponding to a bead position h is obtained from $F_v(h) = d\phi/dh$. In this manner we obtain a flow-force calibration, shown in Fig. 2 *d*.

At this point we have prepared a system with which we can exert a controlled force (in the range ~2–300 pN) on a single molecular attachment for an indefinite time. For the particular application of measuring bond rupture forces, we now subject the bead to progressively faster flows until the bead breaks loose. For the measurements reported here, we used the following series of flow rates: 50, 60, 70, 80, 100, 120, 140, and 160 μl/min. Each flow had 2-s duration with a 5-s intermission between flows. One could, of course, design a different flow versus time scheme (e.g., linearly increasing flow, which would correspond to constant rate of tip retraction in AFM experiments). Passive adsorption couples the BSA molecules to the surfaces sufficiently strongly that they are not ripped off before the biotin-avidin bond breaks (Florin et al., 1994; Allen et al., 1996; Lo et al., 1999; Wong et al., 1999).

In Fig. 2 we give an example of the whole procedure. The measured potential in Fig. 2 *b* is striking in that the constraint on the vertical motion of the bead imposed by the attachment point is clearly visible as a cutoff at $h \approx$ 21 nm. The potential for the free bead would follow the dotted line, which is the DLVO form. The position of this cutoff with respect to the minimum of the potential depends on the details of how the bead is attached. The attachment point generally lies on top of a bump on the surfaces (which are rough at the nanometer scale), and the taller the bump, the larger the cutoff height.

The time series used to calibrate the force (Fig. 2 *c*) shows how the bead tilts toward the plate under the influence of the flows (the first flow is turned on at $t \approx 17$ s). Even a slow flow moves the average position of the bead downwards considerably (from ~11 to ~6 nm in the first calibration point of Fig. 2 *c*), because the initial position is around the minimum of the potential; subsequent incremental flows make the bead reach only a little closer to the plate (from ~6 to ~3 nm for the whole series in Fig. 2 *c*), because the bead is now held up against the steep part of the potential. Therefore, the tilt angle of the bead for the different calibration points varies little, and the relationship between the flow velocity and the vertical force F_v is linear. We also note that the Brownian motion of the bead is much reduced when it is pushed down by the flow, which helps determine the new equilibrium position.

We show this example because it is also interesting from another point of view. The bead actually detached during the fourth "calibration" flow, at $t \approx$ 52 s, as is clear from the much bigger fluctuations for $t > 52$ s (although not shown in the figure, they reach up to ~50 nm, whereas before the bead was confined to $h <$20 nm, see Fig. 2, *a* and *b*). However, it did not detach completely, being still coupled to the plate through a less constraining tether. This is seen from the effect of the fifth and last calibration flow (at $t \approx 60$ s), which does not sweep the bead off but bends it again toward the plate. However, the value of F_v/F_h is considerably smaller for this second attachment point (with the 30 μl/min flow at $t \approx 60$ s, the bead reaches down to approximately the same height as with the 6 μl/min flow at $t \approx 20$ s). Thus, before it broke the stress was essentially all on the first contact. Presumably, this is similar to what happens in retracting an AFM tip through several tens of nanometers in the course of similar force measurements (Wong et al., 1999). For the measurements reported below, two other beads showed similar behavior; the rest detached in a one-step process.

Fig. 2 *d* shows the force calibration for this particular bead. From this and other calibration curves, we see that the accuracy with which we can measure the force on the attachment point is, with the present protocol, of order 10% (for example, for the calibration shown in Fig. 2 *d*, the slope of the fit is 2.13 $\pm$ 0.15 pN/(μl/min)). Given the nonlinear transformation introduced by the potential curve (Fig. 2 *b*), the fact that the measured vertical force comes out proportional to the flow velocity confirms the validity of the method. The upper abscissa scale, although not needed for the force measurements, is added to demonstrate the force amplification effect mentioned earlier. This scale is an estimate of the horizontal drag force F_h that the flow exerts on the bead. The simplest estimate is to calculate the flow velocity u at a position in the flow cell corresponding to the center of the bead (using the known flow rate, cell geometry, and a parabolic velocity profile in the cell), and use this velocity in the Stokes formula $F_{Stokes} = 6\pi\eta uR$, in which η is the viscosity and R the radius of the bead. A better estimate is to use the exact result for a sphere close to a wall in a shear flow (linear velocity profile) (Goldman et al., 1967), which is, for the horizontal force, $F_h = 1.70\ F_{Stokes}$ in the present case (distance to the wall $\ll$ radius of the sphere). In Fig. 2 *d* we use this estimate for F_h; because we have a parabolic velocity profile, the real horizontal force will be somewhat lower (somewhere between F_{Stokes} and $1.7\ F_{Stokes}$). We stress that the precise value does not matter for these measurements, because we see from Fig. 2 *d* that indeed $F_v \gg F_h$; in this example $F_v/F_h \approx 23$. The ratio F_v/F_h varies considerably (by at least a factor of 20) from sample to sample, as it depends on the details of how the bead is attached; for the measurements reported below, the average of this ratio was ~12, the minimum and maximum values were 1 and 32, respectively. This is the mechanism by which adhering beads, or cells, can be detached from a solid substrate by weak lateral forces (i.e., much smaller than the force required to separate a single molecular contact). We can often detach in this way a bead bound to the surface by several contacts, because the attachment points break sequentially, each in turn sustaining essentially the whole strain. We will detail these measurements elsewhere.

Presently, the following are our results for the streptavidin-biotin detachment force. From 25 beads selected according to the criteria mentioned earlier, we obtained nine single-molecule measurements of detachment force. These we list below; recalling that the experiment is performed by applying a series of increasingly faster flows, we give the measurements in the format [lower limit, upper limit], where lower limit is the largest force which did not detach the bead during the 2-s duration of the flow and upper limit is the force which actually detached the bead within 2 s. These are the data:

[35,52], [36,42], [33,37], [38,51], [42,53], [30,37], [33,41], [36,42], [27,34], where the forces are in pN. Of the remaining beads, three were detached by forces clearly smaller than the above range (all <8 pN); we attribute these events to nonspecific sticking. One bead detached in the range [65,109], corresponding presumably to two parallel bonds. For four beads, the detachment force $F_d >$350 pN; presumably, these were sticking through a larger contact area to a damaged part of the surface. For two beads, the value of F_v/F_h was too small to be able to exert the required force with the flow rates we could achieve; for these beads we have only a lower limit for F_d. For two other beads, F_d could not be measured because of a similar effect which we describe below. Finally, four beads gave rise to an unreliable (nonlinear) calibration and were discarded.

We list these events to make the point that many things can go wrong in these measurements; however, one can usually understand what is the problem, so in this sense the system is controlled. For instance, sometimes it happens that as a bead is being pushed down toward the plate by the flow, bumps on the surfaces downstream of the attachment point come into play

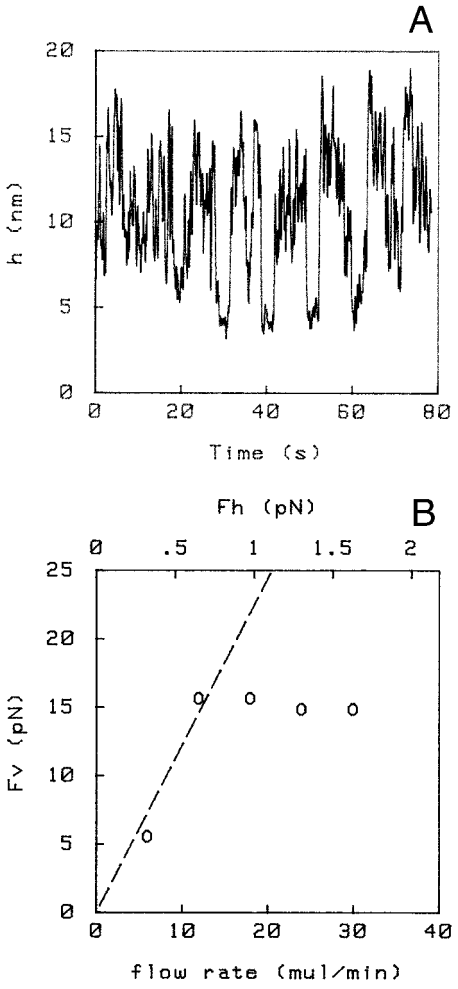

FIGURE 3 This is an example of what can go wrong in the measurements. (*a*) The bead is subjected to a series of 5 flows, as in Fig. 2 *c*. But only the first two produce the expected effect; flows 3, 4, and 5 fail to bring the bead any closer to the slide than it came during flow 2. Apparently, a bump in the surfaces downstream of the attachment point holds the bead up. This is reiterated in the corresponding "calibration curve" (*b*). The last three points do not represent the true vertical force on the attachment point at those flow rates.

and effectively relieve the stress on the attachment point. This was the case for 2 of the 25 beads in our sample, and we show one of these cases in Fig. 3. The first two flows (at $t \sim 20$ s and $t \sim 30$ s) have the expected effect but the subsequent three flows fail to bring the bead any closer to the plate, as if it was leaning on some sort of support. This is obvious from the corresponding values of F_v, shown in Fig. 3 *b*. This bead detached at a flow rate of 60 μl/min, but all that can be said about the corresponding force on the attachment point is that it lies between ~15 pN (Fig. 3 *b*) and the value obtained by extrapolating the dashed line in Fig. 3 *b* to 60 μl/min ($F_v \approx 70$ pN in this case).

Fig. 4 summarizes visually the detachment forces listed above; as the data consist of force intervals, this histogram was built by counting, for each force F_d, the number of datapoints whose interval [lower limit, upper limit] overlaps that force. We conclude that the typical force needed to break the bond (over a 2-s time interval) is 40 ± 10 pN. This seems consistent with the measurements reported in Merkel et al. (1999).

To conclude our gallery of bead behavior, we give two more examples. Fig. 5 shows a case in which the geometry in the neighborhood of the

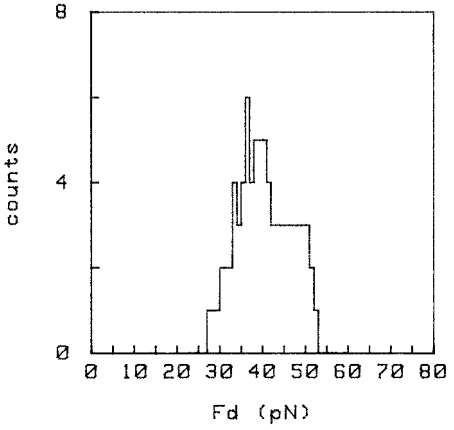

FIGURE 4 Summary of the nine measurements of single biotin-streptavidin bond rupture force obtained. As the data consist of force intervals, this histogram was built by counting the number of intersections of these intervals for a given force.

attachment point is such that the bead's motion is constrained to only a few nanometers; the cutoff in the potential attributable to the attachment point is close to the minimum. Correspondingly, the value of F_v/F_h for this bead was large (≈ 55). Fig. 6 shows that there are soft elements in these beads; sometimes a loose polymer coil protruding from the bead's surface can bridge the gap to the plate and introduce an additional "entropic spring" connection. This is seen in the figure because, rather than a sharp upper cutoff, we have a soft spring (~5 kT over ~20 nm) behavior of the potential; the part of the potential to the right of the minimum is a parabola. We have reported on this effect before and measured the spring constant of these polymer coils (Jensenius and Zocchi, 1997). This behavior is never seen with glass beads.

DISCUSSION AND SUMMARY

The purpose of this paper is twofold. First, we wanted to demonstrate a method, different from the established micromechanical techniques, which allows to exert controlled forces on single molecules; a kind of cantilever-less AFM. For the purpose of measuring bond rupture forces, this

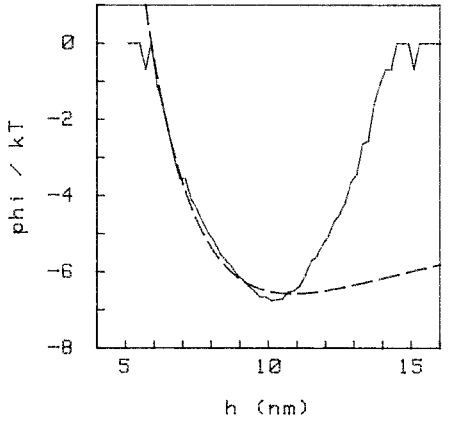

FIGURE 5 A case in which the motion of the bead, although attached at a single point, is very much constrained.

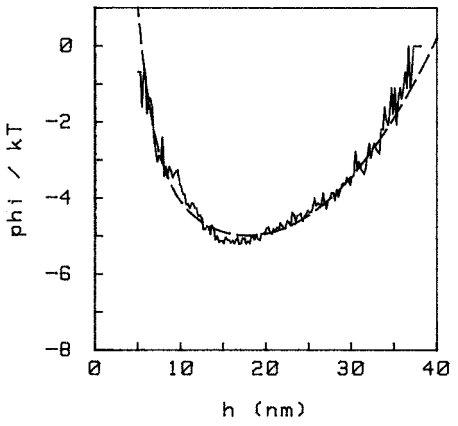

FIGURE 6 This example shows that sometimes loose polymer coils can form soft spring-like connections between bead and slide; instead of a sharp cutoff, the part of the potential to the right of the minimum is a parabola. The dashed line is a DLVO form to the left of the minimum and a parabola to the right.

approach is surely more cumbersome than the AFM or the biomembrane probe, e.g., one needs a calibration for each measurement. However, we think that the interest of the method lies in the possibility that it may allow to exert a nondestructive force on a molecule and simultaneously time monitor nanometer scale conformational motion of the molecule. We are currently working on this aspect.

Second, we tried to present quantitative measurements of the balance of forces involved in detaching adhering beads with lateral forces. We find that a small lateral force typically results in a much larger normal force on the attachment point, in agreement with Chang and Hammer (1996). We also find that the magnitude of this "amplification" effect is highly variable from bead to bead, as it depends on the local (nanometer scale) geometry around the attachment point. Thus, it is questionable whether flow-based cell adhesion assays probe the strength and number of adhesion points, or, on the contrary, some other geometric or elastic property of the cell.

Third, we present measurements of the biotin-streptavidin bond rupture forces for the purpose of exploring how the present approach compares with established techniques. The biotin-avidin and biotin-streptavidin bonds have previously been investigated mechanically by AFM (Florin et al., 1994; Wong et al., 1999) and the micropipette technique of Evans and collaborators (Merkel et al., 1999), where the force transducer is a vesicle or cell. In the AFM measurements, the force required to break a single molecular contact is extracted from a histogram which shows a broad distribution of forces with peaks at multiples of the single molecule value. In the micropipette/biomembrane experiments, conditions are such that single-molecule attachment of the probe can be realized most of the time, which yields a narrower, single-peak distribution of forces. From this point of view, the present technique is similar to the latter experiments, in that we can select beads with only one molecular attachment.

As pointed out by Evans and Ritchie (1997), the force required to disrupt a bond depends (logarithmically) on the pulling rate, because of thermally activated barrier hopping. Therefore the measurements reported here represent only one point in a spectrum of detachment forces. Changing the pulling protocol, e.g., in our case changing the duration of the flows, would yield different F_d values.

REFERENCES

Allen, S., J. Davies, A. C. Dawkes, M. C. Davies, J. C. Edwards, M. C. Parker, C. J. Roberts, J. Sefton, S. J. Tendler, and P. M. Williams. 1996. In situ observation of streptavidin-biotin binding on an immunoassay well surface using an atomic force microscope. *FEBS Lett.* 390:161–164.

Allen, S., J. Davies, M. C. Davies, A. C. Dawkes, C. J. Roberts, S. J. Tendler, and P. M. Williams. 1999. The influence of epitope availability on atomic-force microscope studies of antigen-antibody interactions. *Biochem. J.* 341:173–178.

Block, S. M., L. S. Goldstein, and B. J. Schnapp. 1990. Bead movement by single kinesin molecules studied with optical tweezers. *Nature.* 348: 348–352.

Boland, T., and B. D. Ratner. 1995. Direct measurement of hydrogen bonding in DNA nucleotide bases by atomic force microscopy. *Proc. Natl. Acad. Sci. U.S.A.* 92:5297–5301.

Chang, K. C., and D. A. Hammer. 1996. Influence of direction and type of applied force on the detachment of macromolecularly-bound particles from surfaces. *Langmuir.* 12:2271–2282.

Cluzel, P., A. Lebrun, C. Heller, R. Lavery, J. L. Viovy, D. Chatenay, and F. Caron. 1996. DNA: an extensible molecule. *Science.* 271:792–794.

Coppin, C. M., D. W. Pierce, L. Hsu, and R. D. Vale. 1997. The load dependence of kinesin's mechanical cycle. *Proc. Natl. Acad. Sci. U.S.A.* 94:8539–8544.

Drake, B., C. B. Prater, A. L. Weisenhorn. S. A. Gould, T. R. Albrecht, C. F. Quate, D. S. Cannell, H. G. Hansma, and P. K. Hansma. 1989. Imaging crystals, polymers, and processes in water with the atomic force microscope. *Science.* 243:1586–1589.

Essevaz-Roulet, B., U. Bockelmann, and F. Heslot. 1997. Mechanical separation of the complementary strands of DNA. *Proc. Natl. Acad. Sci. U.S.A.* 94:11935–11940.

Evans, E., and K. Ritchie. 1997. Dynamic strength of molecular adhesion bonds. *Biophys. J.* 72:1541–1555.

Florin, E. L., V. T. Moy, and H. E. Gaub. 1994. Adhesion forces between individual ligand-receptor pairs. *Science.* 264:415–417.

Goldman, A. J., R. G. Cox, and H. Brenner. 1967. Slow viscous motion of a sphere parallel to a plane wall. II. Couette flow. *Chem. Eng. Sci.* 22: 653–660.

Hansma, P. K., J. P. Cleveland, M. Radmacher, D. A. Walters, P. E. Hillner, M. Bezanilla, M. Fritz, D. Vie, H. G. Hansma, C. B. Prater, J. Massie, L. Fukunaga, J. Gurley, and V. Elings. 1999. Tapping mode atomic force microscopy in liquids. Appl. Phys. Lett. 64:1738–1740.

Hinterdorfer, P., W. Baumgartner, H. J. Gruber, K. Schilcher, and H. Schindler. 1996. Detection and localization of individual antibody-antigen recognition events by atomic force microscopy. *Proc. Natl. Acad. Sci. U.S.A.* 93:3477–3481.

Howard, J., A. J. Hudspeth, and R. D. Vale. 1989. Movement of microtubules by single kinesin molecules. *Nature.* 342:154–158.

Israelachvili, J. 1991. Intermolecular and Surface Forces. Academic Press, London.

Jensenius, H., and G. Zocchi. 1997. Measuring the spring constant of a single polymer chain. *Phys. Rev. Lett.* 79:5030–5033.

Kellermayer, M. S., S. B. Smith, H. L. Granzier, and C. Bustamante. 1997. Folding-unfolding transitions in single titin molecules characterized with laser tweezers. *Science.* 276:1112–1116.

Kojima, H., E. Muto, H. Higuchi, and T. Yanagida. 1997. Mechanics of single kinesin molecules measured by optical trapping nanometry. *Biophys. J.* 73:2012–2022.

Lo, Y. S., N. D. Huefner, W. S. Chan, F. Stevens, J. M. Harris, and T. P. Beebe. 1999. Specific interactions between biotin and avidin studied by atomic force microscopy using the Poisson statistical analysis method. *Langmuir.* 15:1373–1382.

Loster, K., and R. Horstkorte, 2000. Enzymatic quantification of cell-matrix and cell-cell adhesion. *Micron.* 31:41–53.

Merkel, R., P. Nassoy, A. Leung, K. Ritchie, and E. Evans. 1999. Energy landscapes of receptor-ligand bonds explored with dynamic force spectroscopy. *Nature.* 397:50–53.

Meyhofer, E., and J. Howard. 1995. The force generated by a single kinesin molecule against an elastic load. *Proc. Natl. Acad. Sci. U.S.A.* 92:574–578.

Noji, H., R. Yasuda, M. Yoshida, and K. Kinosita Jr. 1997. Direct observation of the rotation of F1-ATPase. *Nature.* 386:299–302.

Prieve, D. C., and N. A. Frey. 1990. Total internal reflection microscopy: a quantitative tool for the measurement of colloidal forces. *Langmuir.* 6:396–403.

Prieve, D. C., and Y. J. Walz. 1993. Scattering of an evanescent surface wave by a microscopic dielectric sphere. *Appl. Opt.* 32:1629–1641.

Radmacher, M., M. Fritz, H. G. Hansma, and P. K. Hansma. 1994. Direct observation of enzyme activity with the atomic force microscope. *Science.* 265:1577–1579.

Rief, M., M. Gautel, F. Oesterhelt, J. M. Fernandez, and H. E. Gaub. 1997. Reversible unfolding of individual titin immunoglobulin domains by AFM. *Science.* 276:1109–1112.

Singh-Zocchi, M., Andreasen A., and G. Zocchi. 1999. Osmotic pressure contribution of albumin to colloidal interactions. *Proc. Natl. Acad. Sci. U.S.A.* 96:6711–6715.

Smith, S. B., Y. Cui, and C. Bustamante. 1992. Direct mechanical measurements of the elasticity of single DNA molecules by using magnetic beads. *Science.* 258:1122–1126.

Smith, S. B., Y. Cui, and C. Bustamante. 1996. Overstretching B-DNA: the elastic response of individual double-stranded and single-stranded DNA molecules. *Science.* 271:795–799.

Svoboda, K., and S. M. Block. 1994. Force and velocity measured for single kinesin molecules. *Cell.* 77:773–784.

Svoboda, K., C. F. Smith, B. J. Schnapp, and S. M. Block. 1993. Direct observation of kinesin stepping by optical trapping interferometry. *Nature.* 365:721–727.

Tskhovrebova, L., J. Trinick, J. A. Sleep, and R. M. Simmons. 1997. Elasticity and unfolding of single molecules of the giant muscle protein titin. *Nature.* 387:308–312.

Vale, R. D., T. Funatsu, D. W. Pierce, L. Romberg, Y. Harada, and T. Yanagida. 1996. Direct observation of single kinesin molecules moving along microtubules. *Nature.* 380:451–453.

Viani, M. B., T. E. Scheffer, and A. Chand. 1999. Small cantilevers for force spectroscopy of single molecules. *J. Appl. Phys.* 86:2258–2262.

Wang, M. D., M. J. Schnitzer, H. Yin, R. Landick, J. Gelles, and S. M. Block. 1998. Force and velocity measured for single molecules of RNA polymerase. *Science.* 282:902–907.

Wong, J., A. Chilkoti, and V. T. Moy. 1999. Direct force measurements of the streptavidin-biotin interaction. *Biomol. Eng.* 16:45–55.

Yasuda, R., H. Noji, K. Kinosita Jr., and M. Yoshida. 1998. F1-ATPase is a higly efficient molecular motor that rotates with discrete 120° steps. *Cell.* 93:1117–1124.

Yin, H., M. D. Wang, K. Svoboda, R. Landick, S. M. Block, and J. Gelles. 1995. Transcription against an applied force. *Science.* 270:1653–1657.

Zocchi, G. 1996. Mechanical measurement of the unfolding of a protein. *Europhys. Lett.* 35:633–638.

Zocchi, G. 1997. Proteins unfold in steps. *Proc. Natl. Acad. Sci. U.S.A.* 94:10647–10651.